*Proceedings of the 20th International Conference on Soil Mechanics and Geotechnical Engineering– Rahman and Jaksa (Eds)*


# On the repeated liquefaction during successive shaking table tests.

## Sur la liquéfaction récurrente lors d'essais successifs sur table vibrante.

**Yung-Yen Ko** & Yi-Ting Li
*Department of Civil Engineering, National Cheng Kung University, Taiwan, yyko@ncku.edu.tw*

Chia-Han Chen
*National Center for Research on Earthquake Engineering, National Applied Research Laboratories, Taiwan*

ABSTRACT: Repeated liquefaction of soil in multiple earthquake events has caught our attention in the last decades, such as in the 2010-2011 Canterbury, New Zealand Earthquake sequence. In this study, utilizing a series of shaking table tests on a scale model of an offshore wind turbine, the repeated liquefaction during successive excitations was investigated based on observed excess pore water pressure, acceleration and displacement of the free field of the sandy ground specimen. Results showed that, for an excitation that liquefied the ground specimen moderately, a later onset and smaller extent of liquefaction were observed in the subsequent replicated excitation probably due to the densification of soil. However, for input motions strong enough to liquefy the entire ground specimen, a repetition of the excitation still caused a thorough liquefaction. In addition, the degradation of soil stiffness during liquefaction was revealed using 1-D shear beam idealization to interpret the seismic ground response, and unexpectedly the soil stiffness during a replicated excitation was lower, possibly due to the varied soil fabric after its deposition from a liquefied state.

RÉSUMÉ : La liquéfaction récurrente des sols due à des séismes est observée depuis ces deux dernières décennies, notamment lors du séisme de 2010-2011 à Canterbury, Nouvelle-Zélande. Dans cette étude, en utilisant une table à secousses avec un modèle réduit d'une éolienne offshore, une liquéfaction récurrente a été analysée suite à des excitations successives à partir de la pression excessive d'eau interstitielle ainsi que l'accélération et le glissement du milieu sableux. Pour une excitation ayant conduit à une liquéfaction modérée du milieu, une apparition tardive avec un impact limité de la liquéfaction était observée lors des excitations ultérieures probablement due à la densification du sol. Cependant, lorsque les secousses étaient suffisamment fortes pour liquéfier entièrement le sol, une deuxième opération provoquait toujours une liquéfaction complète. Une dégradation de la rigidité du sol durant la liquéfaction était aussi révélée en utilisant le modèle de cisaillement 1-D pour interpréter la réponse sismique du sol et, de manière inattendue, la rigidité du sol suite à des excitations répétées était plus faible, probablement en raison des couches de structures différentes du sol déposées après liquéfaction.

KEYWORDS: repeated liquefaction; shaking table test; 1-D shear beam idealization; degradation of liquefied soil.

## 1 INTRODUCTION

### 1.1 *Background*

Soil liquefaction is recognized as one of the most hazardous geotechnical phenomena during earthquakes. It causes not only settlement and lateral spreading of the ground, but also soil degradation which may subsequently induce foundation failure.

In recent years, repeated liquefaction at a specific site that experienced multiple strong earthquakes has further caught our attention. A typical example is the 2010-2011 Canterbury, New Zealand earthquake sequence. Widespread repeated liquefaction was observed in suburb of Christchurch city in three relatively major events, the 2010 Mw 7.1 Darfield earthquake (mainshock), the 2011 February Mw 6.2 and 2011 June Mw 6.0 Christchurch earthquakes (aftershocks) (Kiyota et al. 2012), and the situation was even more severe during the 2011 February aftershock than the mainshock (Townsend et al. 2016). Towhata et al. (2014) also reported 26 sites of repeated liquefaction during the 2011 off the pacific coast of Tohoku earthquake.

Concern on repeated liquefaction is inspired by the fact that liquefaction of granular soil could be influenced by factors such as its density and permeability, which might be changed after the deposition of liquefied soil. For example, densification of soft soil layer with 1-m settlement after the repeated liquefactions during the 2010-2011 Canterbury earthquake sequence was revealed by the increase of soil resistance (Kiyota et al. 2012). However, Alberto-Hernandez & Towhata (2017) indicated that the increase of the relative density ($D_r$) of soil due to liquefaction is usually around 10%, which is not enough to reduce the liquefaction potential (Towhata et al. 2013). On the other hand, experimental study of Ye et al. (2007) using successive shaking table tests with the same input motions showed that the densified sandy ground due to liquefaction could be liquefied again in next excitation. However, after the densification due to repeated liquefaction, the ground acceleration was increased, and the dissipation time of excess pore water pressure (EPWP) after liquefaction was decreased.

### 1.2 *Methodology and Objectives*

A series of 1-g shaking table tests on a 1/25 scale model of a jacket-supported offshore wind turbine installed in sandy ground (see Figure 1) were conducted to investigate the influence of soil liquefaction on the seismic response of its superstructure and group piles (Ju et al. 2019). The ground specimen in these tests was prepared using a 2.5 m (L) × 2.5 m (W) × 3.0 m (D) biaxial large laminar shear box as the soil container, which has a flexible boundary composed of layers of movable frames to minimize the boundary effect, enabling a finite-volume ground specimen to approximate the semi-infinite level ground. The 8 m × 8 m high-performance shaking table in the Tainan Laboratory of National Center for Research on Earthquake Engineering (NCREE), Taiwan was utilized, which can accommodate the mentioned large laminar shear box for large-scale seismic simulation of geotechnical physical model. The input motions included 2-Hz sinusoids scaled to various acceleration amplitudes and an actual pulse-like earthquake, and some of the excitations were repeated for different research purposes. During these tests, EPWP and

acceleration in the free field of the ground specimen as well as the displacement of the movable frames were measured, which allowed for the study on the development of liquefaction as well as the characteristics of liquefied ground response.

Taking advantage of these shaking table tests, the repeated liquefaction of the ground specimen subjected to successive excitations was examined by observing the differences between its behaviors during two tests using the same input motion. Focuses are on the EPWP generation and dissipation, the ground response characteristics, the soil degradation in the liquefaction process and the variation of these phenomena during successive excitations. Thus, better understanding of soil liquefaction, its influence factors and consequences can be obtained.

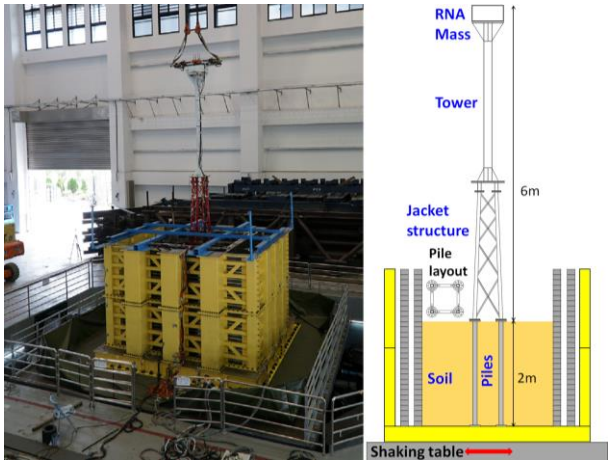


Figure 1. Setup of the investigated shaking table tests of 1/25 scale model of a jacket-supported offshore wind turbine.

## 2 TEST CONFIGURATIONS

The configurations of the mentioned shaking table tests that are related to this study are briefly introduced in this section.

### 2.1 *Sandy ground specimen*

The seabed condition of thick alluvium mainly composed of sand and silt was approximated. Malaysia silica sand with grain sizes from 0.15 mm to 0.425 mm was used. The wet sedimentation method was utilized, and it had been verified to obtain a sandy ground specimen which is satisfactorily homogeneous, almost fully saturated and sufficiently loose to be liquefiable (Ueng et al. 2006). A specimen thickness of 2 m was specified, and the achieved one was 2.03 m. The initial $D_r$ value of the specimen was 11.3% (Ko & Li 2020). However, a 1-g test with a specimen thickness of 2 m is insufficient to account for the overburden stress in the general field conditions so that the test results are only representative of a relatively low overburden situation.

### 2.2 *Instrumentation layout*

The instrumentation layout for the ground specimen is given in Figure 2. Piezometers were deployed in soil at elevations of 1.75 m, 1.50 m, 1.25 m, 1.00 m, 0.75 m, 0.50 m and 0.25 m, i.e. every 0.25 m downward from the ground surface, to monitor the built-up of EPWP. Miniature accelerometers were embedded in soil at elevations of 1.75 m, 1.25 m and 0.75 m. These mentioned sensors were embedded in between the flexible boundary of the shear box and the pile group to be approximated as in the free field. However, the piezometer and accelerometer at EL. 1.25 m malfunctioned. Fortunately piezometers were also installed in the soil between the group piles at EL. 0.75 m, EL. 1.25 m and EL. 1.75 m, and they could serve as alternatives because the EPWP measured here was close to that in the free filed at the same elevation probably due to the large pile spacing (Ko & Li 2020). In addition, the movable frames that form the laminar boundary of the shear box were instrumented by position sensors to give the displacement data that can approximate the ground response.

### 2.3 *Test sequence and input motions*

The sequence of the shaking table tests and corresponding input motions that were investigated herein, which can be divided into two phases, are listed in Table 1. The excitations were applied uniaxially in X-direction (north-south), as defined in Figure 2.

In the first phase, only the ground specimen and the 2×2 pile group model (abbreviated as GP for case ID) were setup to perform pilot tests for easier examination of pile-soil interaction (Ko & Li 2020). Only the 2-Hz sinusoid was used as the input motion in this phase, and acceleration amplitudes included 50 gal and 75 gal, and the achieved table motions are given in Figure 3(a) and Figure 3(b). It is noted that right after the ramp-up stage one or two cycles exceeded the target probably due to the inertial effect of the massive ground specimen along with the shear box.

In the second phase, the full wind turbine model (abbreviated as WT for case ID) was assembled on the pile group, including the jacket substructure, the tower, the steel block representing the mass of rotor-nacelle-assembly (RNA), as shown in Figure 1. Sinusoidal excitation test with amplitudes of 50 gal was also included for comparison with the 50-gal-amplitude pile-group-only case. In addition, a pulse-like actual record from the seismic station nearest to Port of Hualien (HWA062) during the 2018 Hualien, Taiwan earthquake (abbreviated as 2018HWA062 hereafter) was used for earthquake excitation tests. The scaling factor for time $\lambda_T = \sqrt{\lambda} = 5$ was considered to make the acceleration of the model representative of the prototype (Ko & Li 2020), and the achieved table motion during the test is shown in Figure 3(c). Only the cases with a zero period acceleration (ZPA) of 200 gal, in which liquefaction of the entire ground specimen occurred, are discussed in this study.

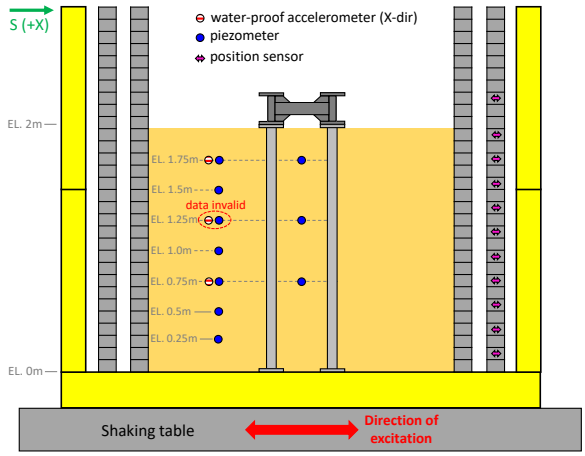


Figure 2. Instrumentation layout of the ground specimen.

Table 1. Test sequence of the investigated shaking table tests

| Case ID | Input motion | ZPA (gal) | $D_r$* (%) | Remarks |
|---|---|---|---|---|
| **Phase 1: ground and pile group model only** | | | | |
| GP-02 | 2-Hz Sinusoid | 50 | 17.8 | Half of ground liquefied |
| GP-03 | 2-Hz Sinusoid | 75 | 31.1 | Entire ground liquefied |
| **Phase 2: full wind turbine model** | | | | |
| WT-02 | 2-Hz Sinusoid | 50 | 34.1 | Less than half ground liquefied |
| WT-07 | 2018HWA062 | 200 | 42.2 | Entire ground liquefied |
| WT-09 | 2018HWA062 | 200 | 47.0 | Entire ground liquefied |

*$D_r$ was calculate by dry bulk density after excitation.

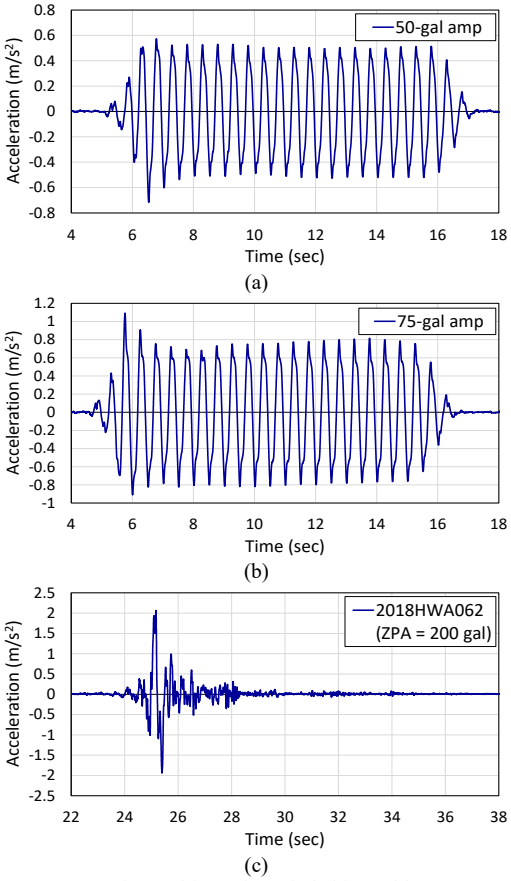


Figure 3. Input motions of investigated shaking table tests: (a) 50-gal amp. 2-Hz sinusoid; (b) 75-gal amp. 2-Hz sinusoid; (c) 2018HWA062.

## 3 RESULTS OF SINUSOIDAL EXCITATION TESTS

### 3.1 *Variation of EPWP*

In this section, variation of EPWP in the free field in terms of excess pore water pressure ratio ($r_u$), namely, the ratio of EPWP to the effective overburden stress ($\sigma_v'$), is examined to reveal the occurrence and extent of liquefaction; when $r_u \approx 1$, soil is considered completely liquefied. It is noted that $r_u$ might be affected by discrepancy between the prescribed and actual elevation of the piezometer in the calculation of $\sigma_v'$ for possible variation of the latter during the tests, yet the prescribed ones were still used because there was no practical way to confirm the actual ones. Thus, values of $r_u$ could be not very close to 1 when soil was liquefied, yet the tendency of $r_u$ curves still helped to determine the occurrence of liquefaction.

Figure 4(a) gives $r_u$ time histories at each instrumented elevation in GP-02 test. $r_u$ increased rapidly during 5-10 sec. at all elevations, reached its maximum at about 10 sec., except at EL. 1.75 m a delay of about 3 seconds was observed, and then kept roughly unchanged during the remains of the excitation. For EL. 1.50 m, EL 1.25 m and EL 1.00 m, maxima of $r_u$ were around 0.90-0.96 and can be considered initial liquefaction. Although $r_u$ at EL. 1.75 m did not exceeds 0.90, EPWP did not dissipate right after the excitation until around 30 sec., implying considerable liquefaction had been induced. The lower $r_u$ at EL. 1.75 m was probably due to the mentioned elevation discrepancy. Besides, EPWP dissipation initiated sooner at greater depths for those liquefied elevations. On the other hand, for elevations no higher than 0.75 m, soil was not liquefied because $r_u \leq 0.7$, and EPWP dissipation occurred right after the shaking. It is concluded that the upper half of the ground specimen reached initial liquefaction after 5 seconds of excitation.

Figure 4(b) shows $r_u$ at all elevations in GP-03 test, which increased sharply at the end of the ramp-up stage of the excitation, probably due to the over-target amplitudes, and reached 0.9-1.0 during the remains of the excitation. Similar to the previous case, the dissipation of EPWP started sooner at greater depths and was generally later in this case except for EL. 0.25 m, where EPWP dissipated right after the cease of excitation. In addition, $r_u$ mildly increased before its dissipation to slightly above 1 at elevations no lower than 1.25 m, implying the gradual settlement of the piezometer. To sum up, almost the entire ground specimen reached complete liquefaction.

In WT-02 test, the input motion was again 50-gal amplitude sinusoid so that its $r_u$ time histories, as shown in Figure 4(c), can be compared with those in GP-02 test. It took nearly twice longer for $r_u$ to reach its maximum at each elevation. Soil was considered liquefied only at EL. 1.50 m and EL 1.75 m at about 14 sec., indicating smaller liquefaction extent (approximately the upmost quarter of the ground specimen), and EPWP started to dissipate seconds earlier, conformable to the finding of Ye et al. (2007). In addition, maximum values of $r_u$ at the non-liquefied elevations were also smaller. It can thus be concluded that the liquefaction severity of the ground specimen became lower after being liquefied twice (partially in GP-02 test and entirely in GP-03 test), and this could be due to the higher density of soil after each deposition from its liquefied state, as exhibited in the $D_r$ values in Table 1, especially the substantial rise after GP-03 test.

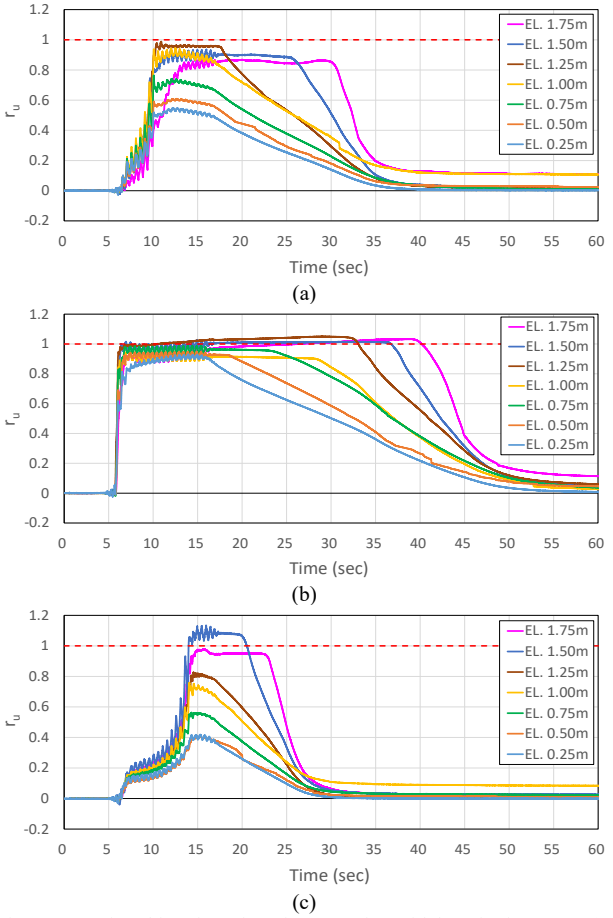


Figure 4. Time histories of $r_u$ in 2-Hz sinusoidal excitation tests: (a) GP-02 (50-gal amp.); (b) GP-03 (75-gal amp.); (c) WT-02 (50-gal amp.).

### 3.2 *Variation of ground acceleration*

For each investigated test, ground accelerations at EL. 1.75 m and EL. 0.75 m will be compared. Figure 5(a) gives the ground

accelerations in GP-02 test. Before liquefaction (around 10 sec.), the acceleration was slightly larger at EL. 0.75 m, indicating that the ground specimen has suppression rather than amplification effect to the 2-Hz excitation. After liquefaction, acceleration amplitude at EL. 1.75 m dropped significantly and exhibited irregular waveform until around 13 sec, and then showed some phase difference with respect to that at EL. 0.75 m, probably caused by the liquefaction of upper half ground specimen; on the other hand, the acceleration amplitude at EL. 0.75 m decreased slightly despite of no liquefaction, implying that upper liquefied layers was influential to the response of underlying layers.

Figure 5(b) shows the ground accelerations in GP-03 test. The acceleration was also larger at EL. 0.75 m in the beginning, and then irregular waveforms with some spikes were noticed at both elevations (especially at EL. 1.75 m) around 6-8 sec., implying the initiation of liquefaction. Afterwards, accelerations at both elevations were lower than the table motion probably because shear waves cannot effectively propagate through liquefied soil. It is noted that after liquefaction intermittent spikes showed at EL. 1.75 m, possibly because of the dilatancy of soil due to very low confining pressure near the ground surface (Ko & Li 2020).

Figure 5(c) shows the ground accelerations in WT-02 test. Unlike in GP-02 test, multi-frequency response showed at EL. 1.75 m before liquefaction (around 14 sec) with considerably smaller amplitude than at EL. 0.75 m, which implied that the soil mechanical properties could have been changed substantially. After liquefaction at EL. 1.75 m, irregular waveform and spikes were also noticed; while at EL. 0.75 m (no liquefaction here), the response kept nearly unchanged possibly because of the lower EPWP at this elevation and smaller extent of overlying liquefied layer than in GP-02 test. Hence, repeated liquefaction also has considerable influence on the excited response of the ground.

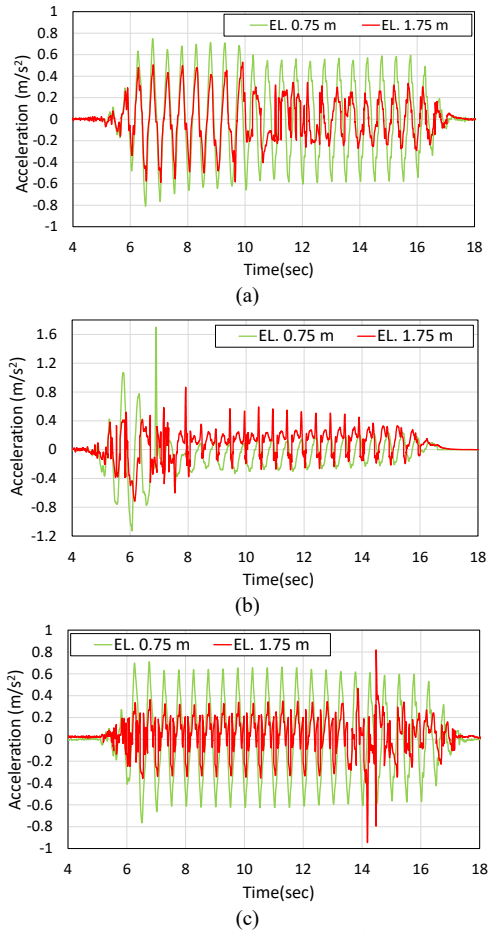


Figure 5. Ground accelerations in 2-Hz sinusoidal excitation tests: (a) GP-02 (50-gal amp.); (b) GP-03 (75-gal amp.); (c) WT-02 (50-gal amp.).

### 3.3 *Strain and stress of soil*

The seismic ground response is usually simplified as the vertical propagation of shear horizontal (SH) waves in semi-infinite horizontally layered soil, which can be regarded as 1-D soil column. Thus, 1-D shear beam idealization proposed by Koga & Matsuo (1990) can be used to estimate the shear stress and strain of soil from the measured ground response in terms of displacement or acceleration. Based on the idealized and discretized 1-D shear beam as shown in Figure 6, the shear stress at the depth of $x_i$, $\tau_i$, can be estimated as follows:

$$\tau_i(t) = \tau_{i-1}(t) + \rho \frac{a_{i-1}+a_i}{2}(x_i - x_{i-1}) \quad (1)$$

where $\rho$ is the mass density of soil; $a_i$ is the acceleration at $x_i$.

In addition, the shear strain at the depth of $x_i$, $\gamma_i$, can be estimated in the finite difference form:

$$\gamma_i(t) = \frac{[u_{i+1}(t)-u_i(t)]\frac{\Delta x_{i-1}}{\Delta x_i}+[u_i(t)-u_{i-1}(t)]\frac{\Delta x}{\Delta x_{i-1}}}{\Delta x_i+\Delta x_{i-1}} \quad (2)$$

where $\Delta x_i = x_{i+1} - x_i$; $u_i$ denotes the displacement at $x_i$

Utilizing the free surface condition ($\tau_1 = 0$), the shear stresses at different depths can be calculated sequentially using Eq. 1 if the acceleration at each concerned depth is known, and the shear strains can also be calculated using Eq. 2 from the directly measured displacements or the double time integration of accelerations (e.g. Zeghal & Elgamel 1994; Ko & Chen 2020).

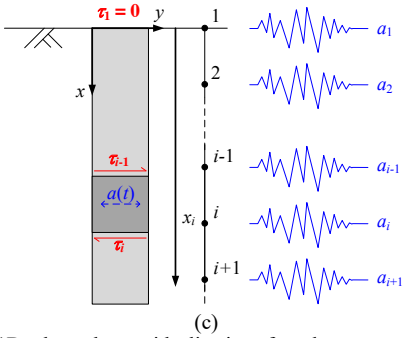


Figure 6. 1D shear beam idealization for shear stress and strain estimation.

Figure 7(a) depicts the stress-strain loops in GP-02 tests from the initiation of excitation to the onset of liquefaction (5-10 sec.). The slope of the loops at EL. 1.75 m gently decreased in the beginning as the shear strain gradually increased and finally dropped to a quite low value as the sudden rise of shear strain, showing that soil had lost its stiffness as a result of liquefaction. As for EL. 0.75 m, where no liquefaction occurred, only gradual and limited degradation soil stiffness was noticed. Besides, its slope was obviously higher than at EL. 1.75 m, exhibiting the contribution of overburden stress to the stiffness of granular soil.

The stress-strain loops in GP-03 tests from the initiation of excitation to the onset of liquefaction (4-7 sec.) are shown in Figure 7 (b). The slope of the loop at both elevations decreased rapidly, and meanwhile its shape was getting irregular, probably due to fast development of liquefaction during the ramp-up stage of the excitation that weakened the soil quickly. Figure 7(c) shows the stress-strain loops in WT-02 tests from the initiation of excitation to the onset of liquefaction (5-14 sec.). The tendency was somewhat similar to that in GP-02 test, yet the loops at EL. 1.75 m had smaller slope in the beginning and were more distorted with larger shear strain amplitudes as approaching liquefaction, implying lower soil stiffness in liquefied layer during the excitation; while at EL. 0.75 m slightly less soil

degradation was noticed, possibly corresponding to its lower EPWP and smaller extent of upper liquefied layer.

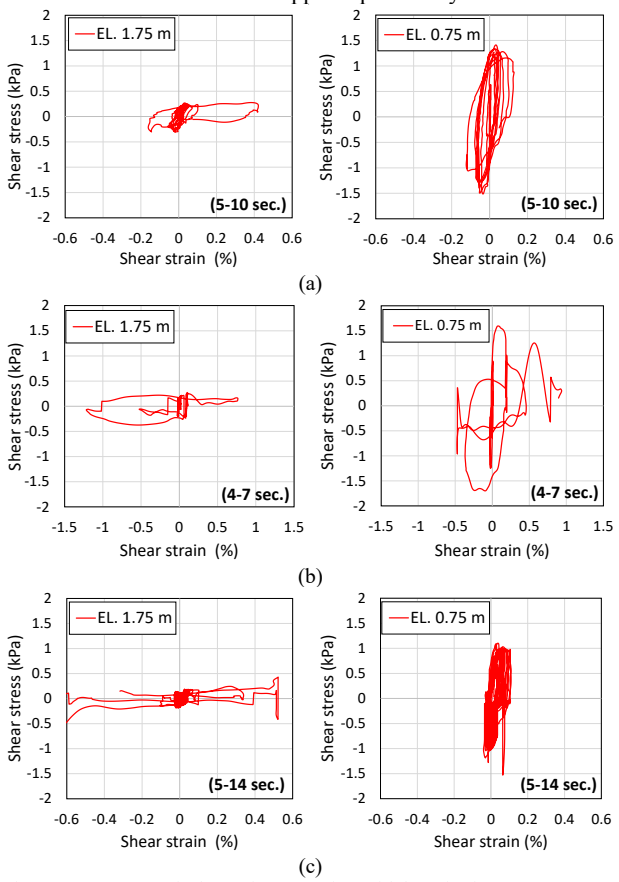


Figure 7. Stress-strain loops in 2-Hz sinusoidal excitation tests: (a) GP-02 (50-gal amp.); (b) GP-03 (75-gal amp.); (c) WT-02 (50-gal amp.).

Based on the stress-strain loops in Figure 7, the equivalent linear shear modulus $G_{eq}$ can be estimated, and its drease with the cyclic shear strain amplitude ($\gamma_{cyc}$) can be thus assessed. Figure 8 compares $G_{eq}$ versus $\gamma_{cyc}$ plots in GP-02 and WT-02 tests. However, it is surprising to notice generally lower $G_{eq}$ values in WT-02 test than in GP-02 test at both EL. 1.75 m and EL. 0.75 m despite the ground specimen was much denser in WT-02 test and the liquefaction was less severe. A speculation of the cause is the considerable change of soil fabric after its deposition from a liquefied state, yet it needs further study in the future for verification

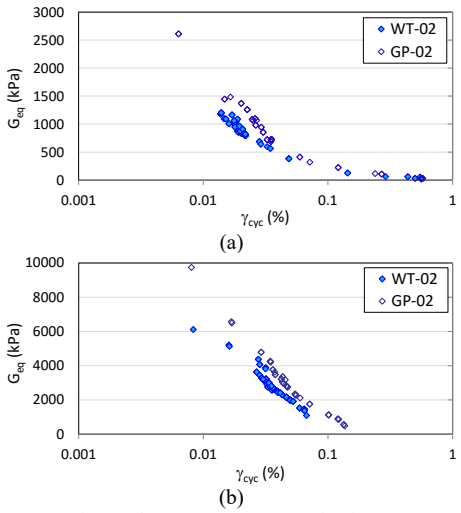


Figure 8. Comparison of $G_{eq}$ versus $\gamma_{cyc}$ plot in GP-02 and WT-02 tests: (a) at EL. 1.75 m; (b) at EL. 0.75 m.

## 4 RESULTS OF EARTHQUAKE EXCITATION TESTS

### 4.1 *Variation of EPWP*

Figure 9(a) shows variation of EPWP in terms of $r_u$ in WT-07 test. $r_u$ at all elevations built up extremely rapidly right after 25 sec, the onset of the acceleration impulse in the input motion shown in Fig. 3(c), and nearly the entire ground was considered liquefied around 26 sec.

Results in WT-09 test are given in Figure 9(b), of which the tendency is similar to those in WT-07 test. Unlike GP-02 and WT-02 sinusoidal excitation tests, repeated liquefaction in this case caused no slower EPWP generation so that nearly the entire ground was still liquefied at about 26 sec. This is probably due to the much intense and pulse-like excitation as well as the smaller difference in density ($D_r$ = 47% in WT-09 and 42% in WT-07). However, the EPWP dissipation was generally seconds earlier, implying the slightly less severity of liquefaction.

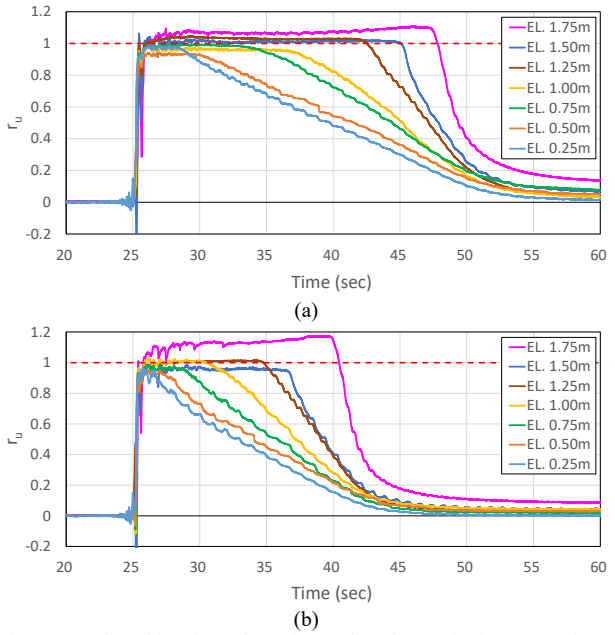


Figure 9. Time histories of $r_u$ in earthquake excitation tests (input motion: 2018HWA062, ZPA = 200 gal): (a) WT-07; (b) WT-09.

### 4.2 *Variation of ground acceleration*

Figure 10 shows the ground accelerations at EL. 1.75 m and EL. 0.75 m of the examined earthquake excitation tests. Despite of the random nature of the earthquake motions, the substantial change of the ground vibration characteristics posterior to liquefaction is still observed. The ground accelerations were generally lower than the table motion after nearly entire ground specimen was liquefied, especially at EL. 1.75 m, where however some spikes possibly related the soil dilatancy near the ground surface showed up as in sinusoidal excitation tests; additionally, the high frequency response was suppressed. These phenomena can be owing to the loss of stiffness and the consequent liquid-like feature of liquefied soil. In general, if the spikes are ignored, the ground accelerations in these two tests are similar.

### 4.3 *Strain and stress of soil*

Similarly, Eq. 1 and Eq. 2 were used to obtain the stress-strain relationship of soil at EL. 1.75 m and EL. 0.75 m. Because the acceleration amplitude kept changing during the earthquake excitation due to its random nature, focus here is only on the significant built-up stage of EPWP (25-26 sec.) in both tests, as shown in Figure 11. Because of the long-duration pulses of the excitation in WT-07 test, approximately one strain-stress loop is

shown in Figure 11(a) at both elevations, and it is quite distorted due to the rapid EPWP rise that caused substantial degradation of soil within this loop. Regrading WT-09 test, similarly only one distorted loop was caused at each elevation, as shown in Figure 11(b); however, the stress level is lower while the strain level is larger, implying lower stiffness subjected to the same excitation after repeated liquefaction even with higher density.

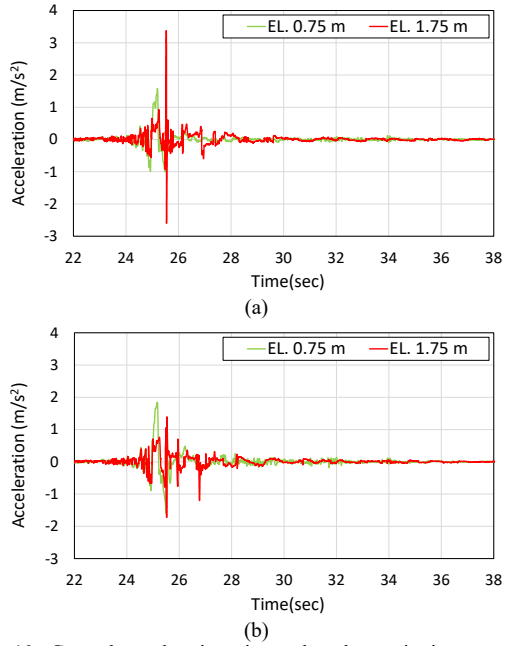


Figure 10. Ground accelerations in earthquake excitation tests (input motion: 2018HWA062, ZPA = 200 gal): (a) WT-07; (b) WT-09.

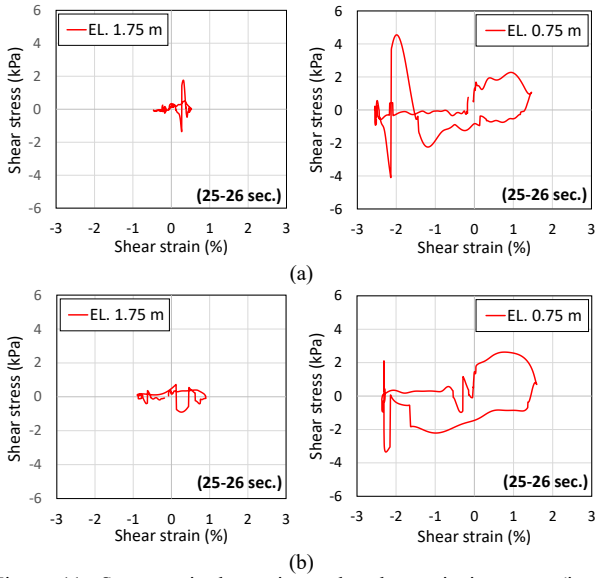


Figure 11. Stress-strain loops in earthquake excitation tests (input motion: 2018HWA062, ZPA = 200 gal): (a) WT-07; (b) WT-09.

## 5 CONCLUSIONS

This study investigated the influence of repeated liquefaction on the seismic ground response via shaking table tests using a large laminar shear box to prepare a liquefiable ground specimen. Based on the findings, the following conclusions are drawn:

Based on different sinusoidal excitation tests with the same acceleration amplitude that liquefied part of the ground specimen, repeated liquefaction reduced severity of liquefaction because soil was denser after it deposited from a liquefied state. However, for an earthquake excitation strong enough to liquefy entire ground specimen, a repetition still caused thorough liquefaction.

In both sinusoidal and earthquake excitation tests, the ground acceleration was much reduced after liquefaction, possibly due to limited shear waves propagation through liquefied soil.

Based on 1-D shear beam idealization, the shear stress and strain of soil were obtained using the measured ground acceleration and displacement. The results indicated the significant increase of shear strain level close to the onset of liquefaction as well as the soil degradation during the excitation.

Although the soil was densified after repeated liquefaction, surprisingly its stiffness during a replicated excitation was lower. The reason is presumed that the soil fabric was much changed after post-liquefaction deposition.

## 6 ACKNOWLEDGEMENTS

The authors gratefully acknowledge the financial support from Ministry of Science and Technology, Taiwan (Research Project MOST 106-3114-F-492-005).

## 7 REFERENCES

Alberto-Hernandez, Y., and Towhata, I., 2017. New insight in liquefaction after recent earthquakes: Chile, New Zealand and Japan. In: Zouaghi, T. (Ed.), *Earthquakes - Tectonics, Hazard and Risk Mitigation*, IntechOpen Limited, London, 117-137.

Ju, S.H., Huang, B.Y., Ni, S.H., Liu, K.Y., Ko, Y.Y., Hsu, S.Y., Chang, Y.W., Lu, L.Y., and Lin, G.L., 2019. Brief introduction of shaking table test of 1/25 scale model of offshore wind turbine with jacket foundation. *International Conference in Commemoration of 20th Anniversary of the 1999 Chi-Chi Earthquake*, Taipei, Taiwan.

Kiyota, T., Yamada, S., and Hosono, Y., 2012. Repeated liquefaction observed during the 2010-2011 Canterbury earthquakes. *Bulletin of ERS* 45, 115-121.

Ko, Y.Y., and Chen, C.H., 2020. On the variation of mechanical properties of saturated sand during liquefaction observed in shaking table tests. *Soil Dynamics and Earthquake Engineering* 129, 105946.

Ko, Y.Y., and Li, Y.T., 2020. Response of a scale-model pile group for a jacket foundation of an offshore wind turbine in liquefiable ground during shaking table tests. *Earthquake Engineering and Structural Dynamics* 49(15), 1682-1701.

Koga, Y, and Matsuo, O., 1990. Shaking table tests of embankments resting on liquefiable sandy ground. *Soils and Foundations* 30(4), 162-174.

Towhata, I., Goto, S., Taguchi, Y., and Aoyama, S., 2013. Liquefaction consequences and learned lessons during the 2011 Mw = 9 gigantic earthquake. *Indian Geotechnical Journal* 43(2), 116-126.

Townsend, D., Lee, J.M., Strong, D.T., Jongens, R., Lyttle, B.S., Ashraf, S., Rosser, B. , Perrin, N., Lyttle, K., Cubrinovski, M., Taylor, M.L., Hughes, M.W., Wilson, T., Almond, P., Jacka, M., McCahon, I., and Christensen, S., 2016. Mapping surface liquefaction caused by the September 2010 and February 2011 Canterbury earthquakes: a digital dataset. *New Zealand Journal of Geology and Geophysics* 59(4), 496-513.

Towhata, I., Maruyama, S., Kasuda, K., Koseku, J. Wakamatsu, K., Kiku, H., Kiyota, T., Yasuda, S., Taguchi, Y., Aoyama, S., and Hayashida, T., 2014. Liquefaction in the Kanto region during the 2011 off the pacific coast of Tohoku earthquake. *Soils and Foundations* 54(4), 859-873.

Ye, B., Ye, G., Zhang, F., and Yashima, A., 2007. Experiment and numerical simulation of repeated liquefaction-consolidation of sand. *Soils and Foundations* 47(3), 547-558.

Ueng, T.S., Wang, M.H., Chen, M.H., Chen, C.H., and Peng, L.H., 2006, A large biaxial shear box for shaking table tests on saturated sand. *Geotechnical Testing Journal* 29(1),1-8.

Zeghal, M., and Elgamel, A.W., 1994. Analysis of site liquefaction using earthquake records. *Journal of Geotechnical Engineering* 120(6), 996-1017.